Experimental section

Materials.

Four tungstophosphates (PW): $[PW_{12}O_{40}]^{3-}$ (PW_{12}) was purchased directly from Sigma-Aldrich and used without further treatment, while $[P_2W_{18}O_{62}]^{6-}$ (P_2W_{18}),[1] $[NaP_5W_{30}O_{110}]^{14-}$ (P_5W_{30}),[2] and $[H_7P_8W_{48}O_{184}]^{33-}$ (P_8W_{48})[3] were prepared according to the literature method and identified by IR spectra and cyclic voltammetry. Poly(sodium-p-styrenesulfonate) (PSS) (MW 70000), poly(ethyleneimine) (PEI) (MW 750,000) and tris(1,10-phenanthroline) ruthenium (Ruphen) were purchased from Sigma-Aldrich and used without further treatment. Other reagents were of AR grade. Water was purified using a Millipore Milli-Q water purification system.

Preparation of four composite films.

For comparison purpose, four composite films (PEI/PW/Ruphen/PSS)n (PW: PW_{12}, P_2W_{18}, P_5W_{30}, P_8W_{48}) were prepared by layer-by-layer self-assembly method based on the electrostatic interaction between each species. Quartz substrates and indium tin oxide (ITO)-coated glasses were cleaned according to a literature procedure.[4] First, substrates were dipped into PEI solution for 20 min to make the surface positively charged because the surface of the substrates is negatively charged, followed by washing with deionized water and drying in nitrogen stream. Then, the positively charged substrate-supported precursor films were alternately dipped into the PW solution (PW is negatively charged), the Ruphen solution (Ruphen is positively charged) and PSS solution (PSS is negatively charged) for 20 min, respectively, and rinsed with deionized water after each dipping. Finally, four composite films

(PEI/PW/Ruphen/PSS)n were obtained by repeating these procedures (n is the deposited number of layers). The self-assembly processes of four composite films (PEI/PW/Ruphen/PSS)n are illustrated in Scheme S1.

Characterization of four composite films.

UV−vis absorption spectra of quartz-supported films were recorded on a VARIAN Cary 50 UV−visible spectrophotometer. The fluorescence spectra of ITO-supported films were recorded on a FLS980 spectrofluorophotometer. Atomic force microscopy (AFM) measurements were performed in air with a SPVA 400 instrument. X-ray photoelectron spectroscopy (XPS) was measured on the ITO using an ESCALAB MK II Surface Analysis System (including X-ray photoelectron spectrometer) with aluminum Kα (1486.6 eV) as the X-ray source. All electrochemical experiments were performed on a CHI660C Electrochemical Workstation (Shanghai Chenhua Instrument Corp., China) at room temperature. A three-electrode system was employed in a quartz cell with a Ag/AgCl (saturated KCl) electrode as the reference electrode, a platinum foil as the counter electrode, and the composite films modified ITO glass as the working electrode.

Reference:

1 W. G. Klemperer, *Inorg. Synth*., 1990, **27**, 71.

2 I. Creaser, M. C. Heckel, R. J. Neitz and M. T. Pope, *Inorg. Chem*., 1993, **32***,* 1573.

3 (a) R. Contant and A. Tézé, *Inorg. Chem.*, 1985, **24**, 4610; (b) R. Contant, *Inorg. Synth*., 1990, **27**, 104.

4 S. Q. Liu, D. G. Kurth, B. Bredenkötter and D. Volkmer, *J. Am. Chem. Soc*., 2002, **124**, 12279.

Table S1. The relationship between the fluorescence quenching efficiencies and the structures of PW.

	Film 1	Film 2	Film 3	Film 4
Charge of PW	-3	-6	-14	-33
Size of PW (nm)	1.0×1.0×1.0	1.0×1.0×1.2	1.5×1.5×1.0	2.0×2.0×1.0
n	4	6	10	16
$\varepsilon_{\text{reduced PW}}$ ($L \cdot mol^{-1} \cdot cm^{-1}$)	9.4×10^3	1.43×10^4	1.84×10^4	2.34×10^4
Γ (PW) (mol/cm^2)	8.3×10^{-11}	2.5×10^{-10}	1.5×10^{-10}	4.0×10^{-11}
Γ (Ruphen) (mol/cm^2)	1.4×10^{-10}	2.2×10^{-10}	2.0×10^{-10}	1.6×10^{-10}
R = Γ (PW) / Γ(Ruphen)	0.58	1.15	0.75	0.24
D (%)	7.8	58.5	73.0	42.8
η	0.13	0.51	0.97	1.78

Note: Film 1: $[PEI/PW_{12}/Ruphen/PSS]_{15}$; Film 2: $[PEI/P_2W_{18}/Ruphen/PSS]_{15}$; Film 3: $[PEI/P_5W_{30}/Ruphen/PSS]_{15}$; Film 4: $[PEI/P_8W_{48}/Ruphen/PSS]_{15}$. n: total reduced electrons of PW in solutions; Γ: the average surface coverages, $\Gamma = N_A A_\lambda / 2m\varepsilon_\lambda$, N_A – Avogadro's constant, A_λ – the absorbance at wavelength λ, m – the number of layers, ε_λ – the isotropic molar extinction coefficient at wavelength λ; R: The ratio of the average surface coverages of PW and Ruphen; D: fluorescence quenching degree, $D = (A_{+E} - A_{-E})/A_{+E} \times 100\%$, A is normalized integral fluorescence area; η: the energy transfer efficiency, η = D/R; ε: the maximum molar extinction coefficient of the electroreduced PW in solutions.

Table S2. The roughness of three composite films PEI/PW, $[PEI/PW/Ruphen/PSS]_3/PEI/PW$ and $[PEI/PW/Ruphen/PSS]_3/PEI/PW/Ruphen$ in scanning range of 5 micrometer.

PW	a	b	c
PW_{12}	1.960 nm	2.388 nm	3.305 nm
P_2W_{18}	1.427 nm	2.287 nm	4.818 nm
P_5W_{30}	1.395 nm	1.933 nm	3.887 nm
P_8W_{48}	1.189 nm	2.283 nm	3.348 nm

Note：(a) film PEI/PW; (b) film $[PEI/PW/Ru(phen)/PSS]_3/PEI/PW$ and (c) $[PEI/PW/Ruphen/PSS]_3/PEI/PW/Ruphen$.

Table S3. The roughness of three composite films PEI/PW, $[PEI/PW/Ruphen/PSS]_3$ /PEI/PW and $[PEI/PW/Ru(phen)/PSS]_3$/PEI/PW/Ru(phen) in scanning range of 1 micrometer.

PW	a	b	c
PW_{12}	1.386 nm	2.297 nm	3.323 nm
P_2W_{18}	1.157 nm	2.180 nm	4.398 nm
P_5W_{30}	1.077 nm	1.779 nm	3.459 nm
P_8W_{48}	0.976 nm	1.959 nm	2.884 nm

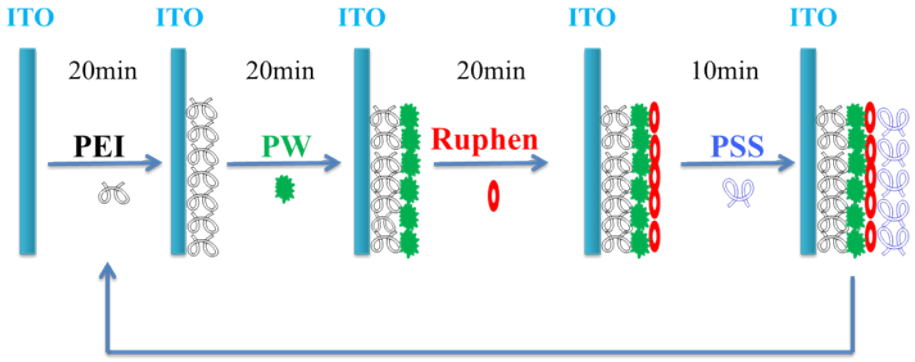

Scheme 1. The layer-by-layer self-assembly process of four composite films (PEI/PW/Ruphen/PSS)n.

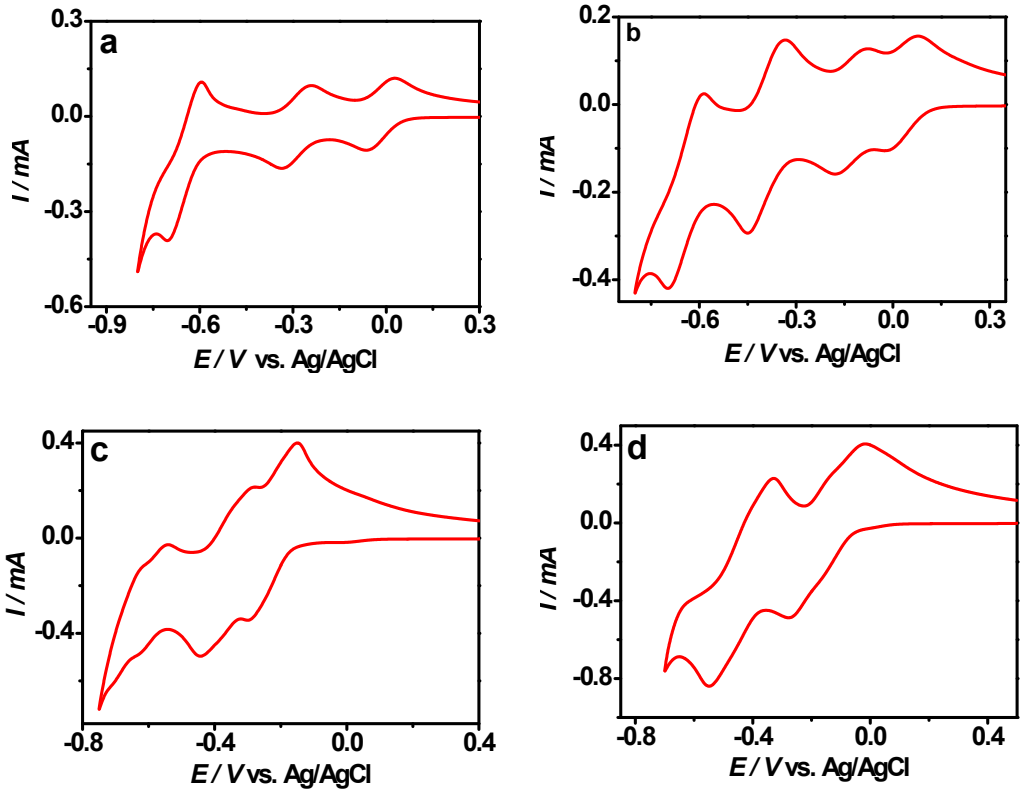

Fig. S1. CVs of (a) PW_{12} (0.5 mM), (b) P_2W_{18} (0.5 mM), (c) P_5W_{30} (0.5 mM) and (d) P_8W_{48} (0.5 mM) in 0.5 M H_2SO_4 solutions using ITO electrode as a working electrode with scan rate of 100 $mV \cdot s^{-1}$.

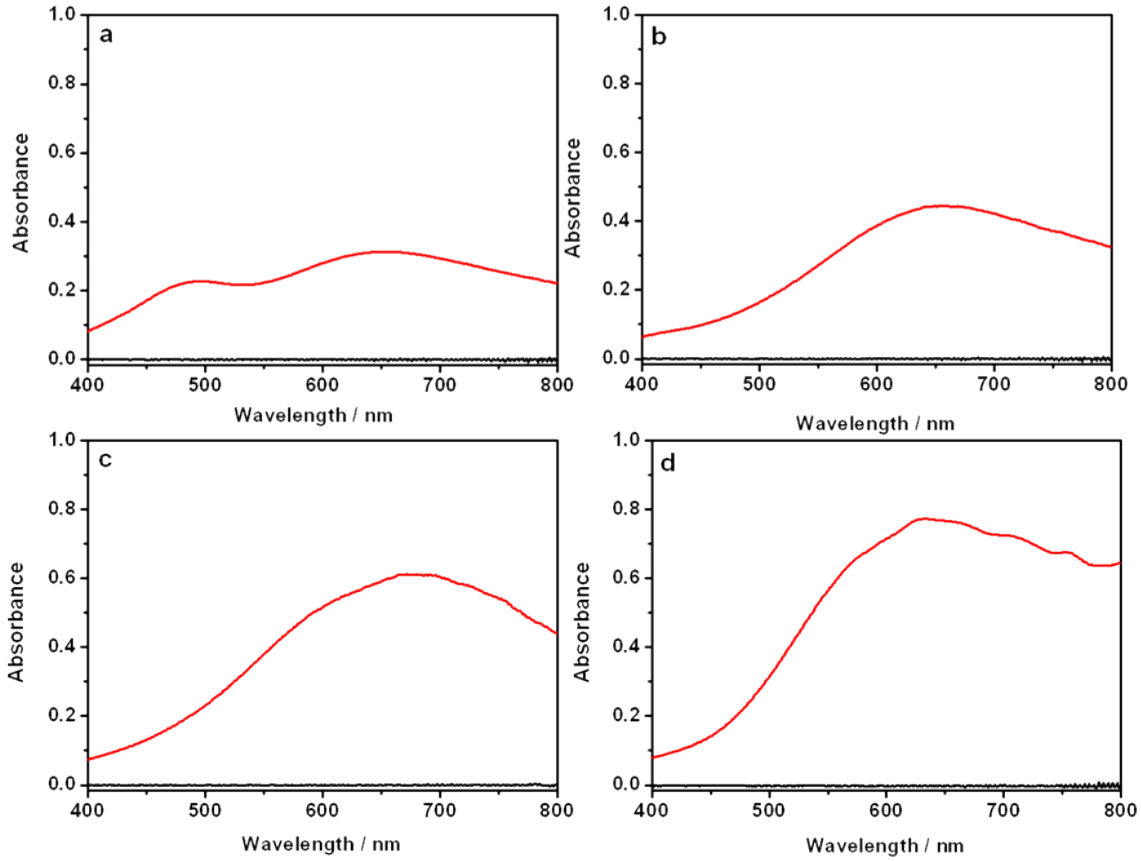

Fig. S2. UV-vis absorption spectra of PW ($3*10^{-5}$M) in 0.5 M Na_2SO_4 + H_2SO_4 (pH 2.5) under electrochemical reduction potential of -0.85V for 1h (red curves): (a) PW_{12}; (b) P_2W_{18}; (c) P_5W_{30}; (d) P_8W_{48} and open circuit (black curves).

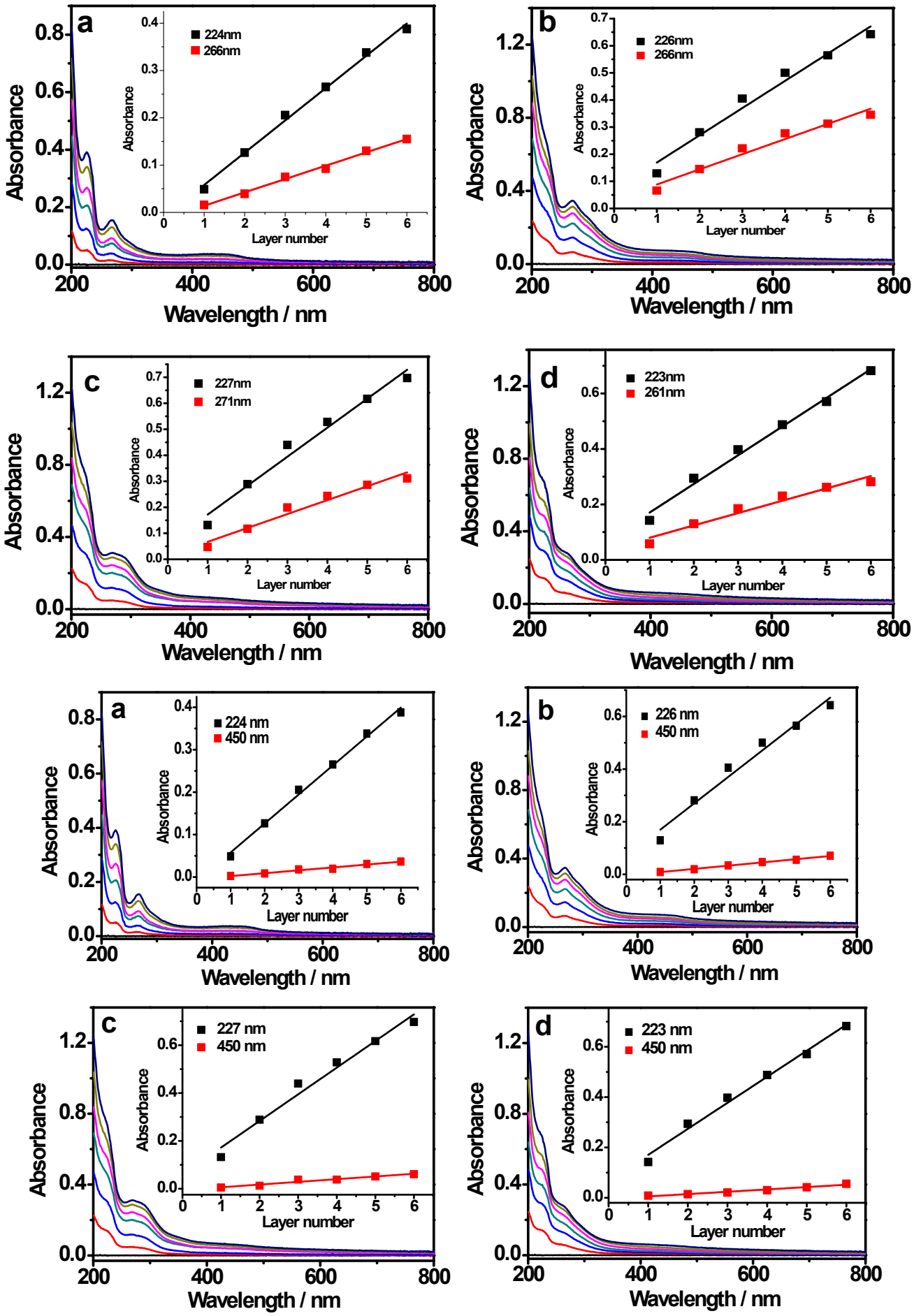

Fig. S3. UV-vis absorption spectra of four composite films (PEI/PW/Ruphen/PSS)n (n = 1-6), the insets show the absorbance vs. the number of layers. (a) PW_{12}; (b) P_2W_{18}; (c) $P_5W_{30;}$ (d) P_8W_{48}.

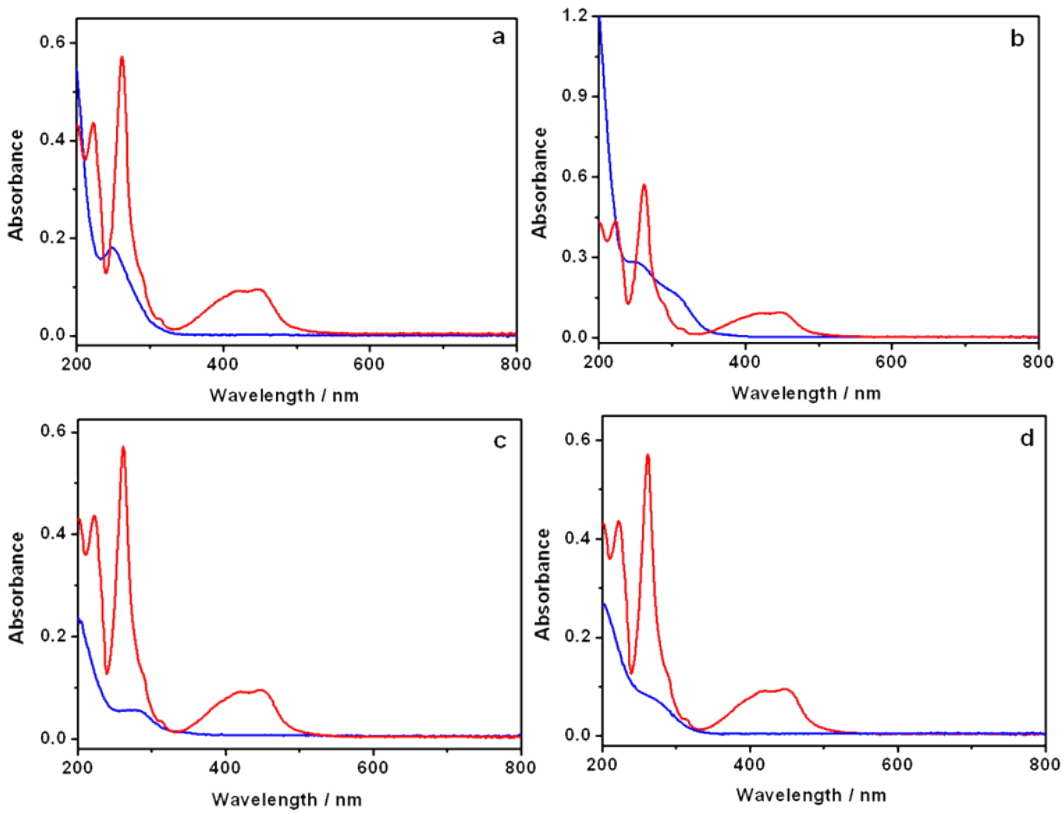

Fig. S4. UV-Vis absorption spectra of PW (blue curves) and Ruphen (red curves) in aqueous solutions. (a) PW_{12}; (b) P_2W_{18}; (c) P_5W_{30}; (d) P_8W_{48}.

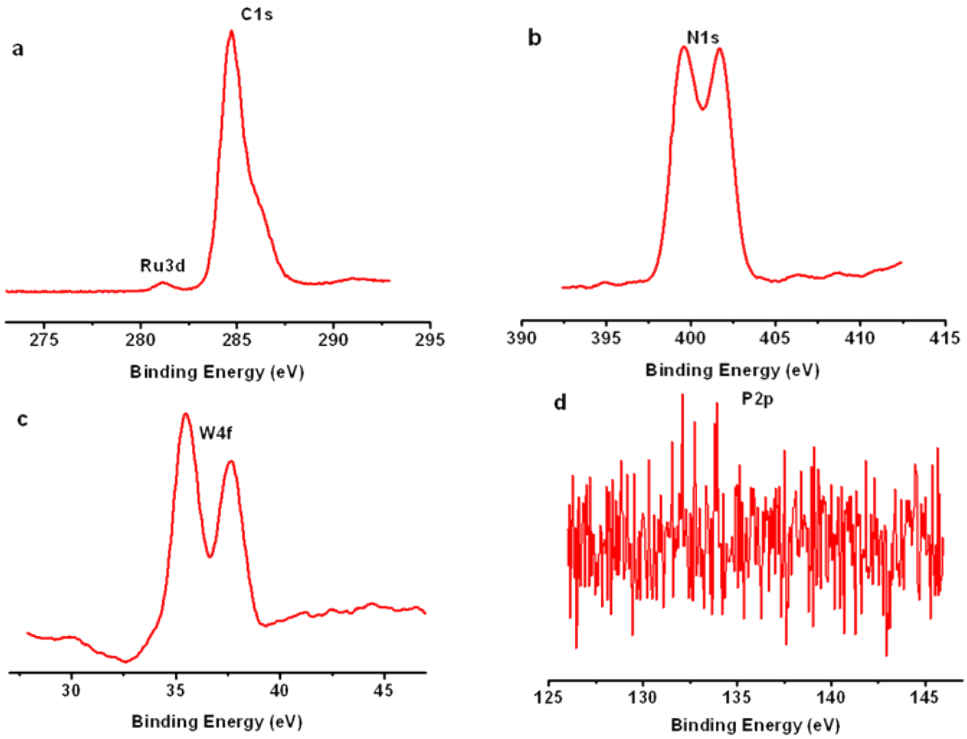

Fig. S5. XPS spectra of the composite film $(PEI/PW_{12}/Ruphen/PSS)_{15}$.

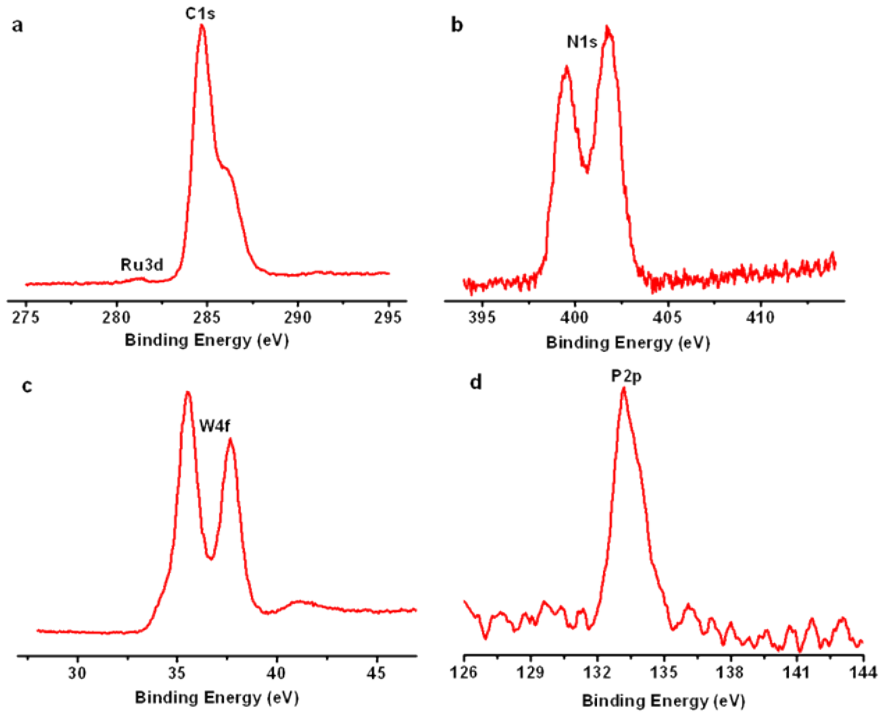

Fig. S6. XPS spectra of the composite film $(PEI/P_2W_{18}/Ruphen/PSS)_{15}$.

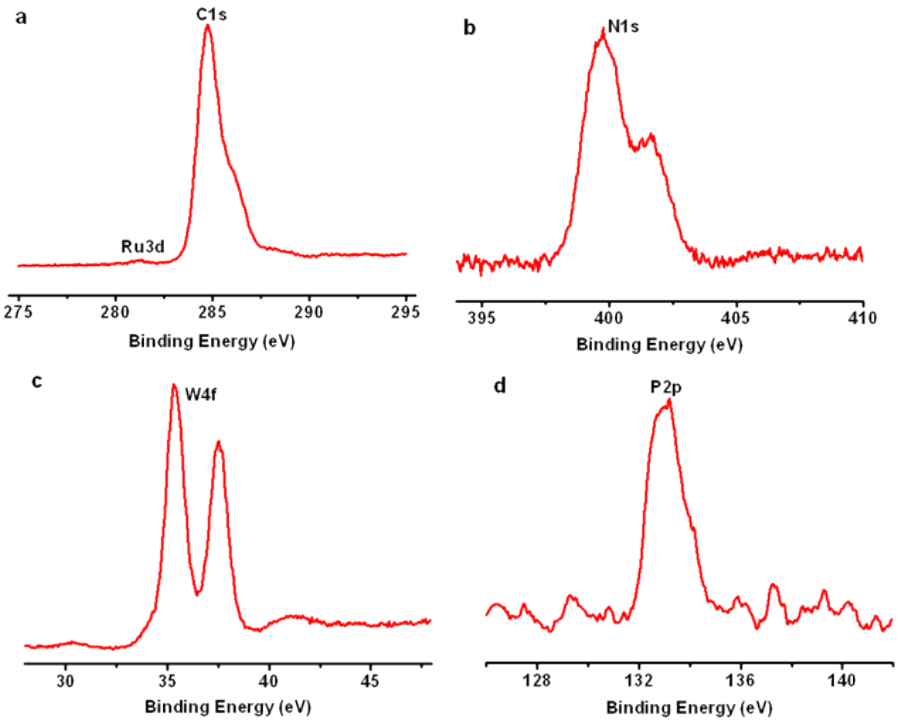

Fig. S7. XPS spectra of the composite film $(PEI/P_5W_{30}/Ruphen/PSS)_{15}$.

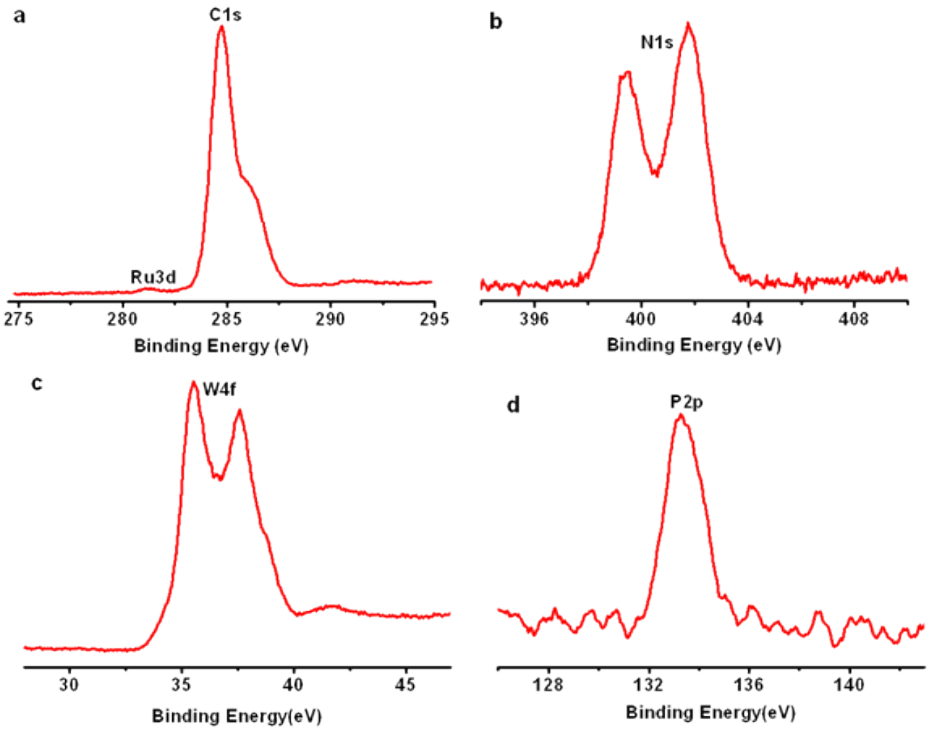

Fig. S8. XPS spectra of the composite film $(PEI/P_8W_{48}/Ruphen/PSS)_{15}$.

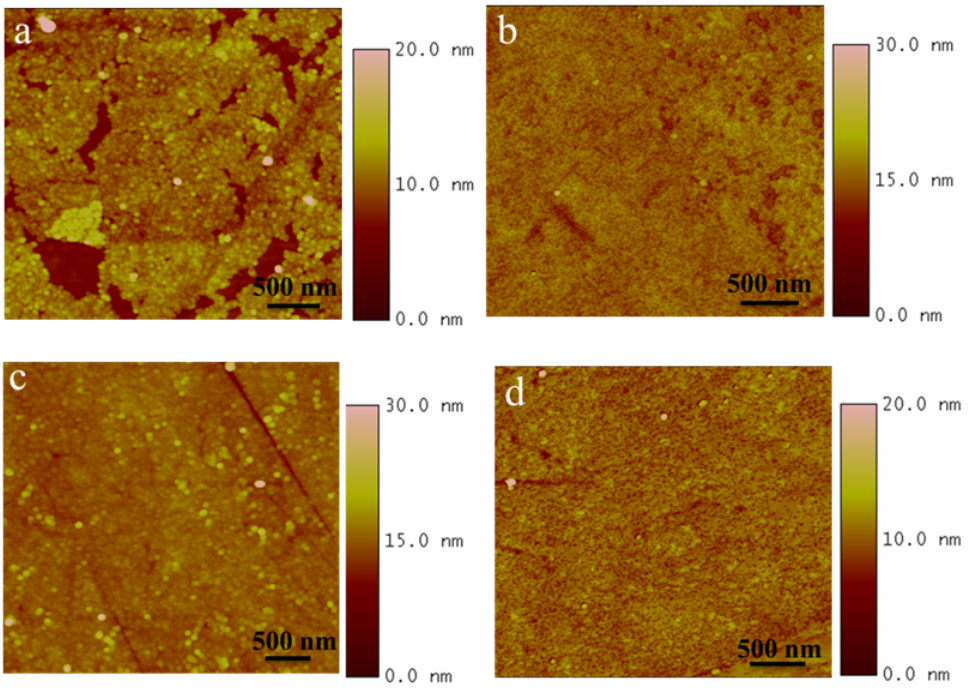

Fig. S9. AFM images of four composite films $[PEI/PW]_1$ on quartz substrates: (a) PW_{12}; (b) P_2W_{18}; (c) P_5W_{30} and (d) P_8W_{48} in scanning range of 5 micrometer.

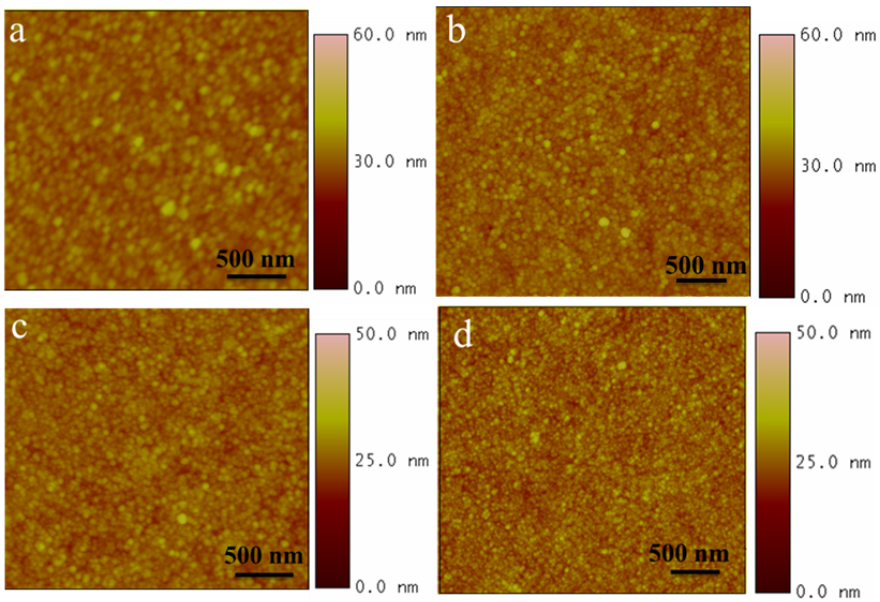

Fig. S10. AFM images of four composite films $[PEI/PW/Ruphen/PSS]_3/PEI/PW$ on quartz substrates: (a) PW_{12}; (b) P_2W_{18}; (c) P_5W_{30} and (d) P_8W_{48} in scanning range of 5 micrometer.

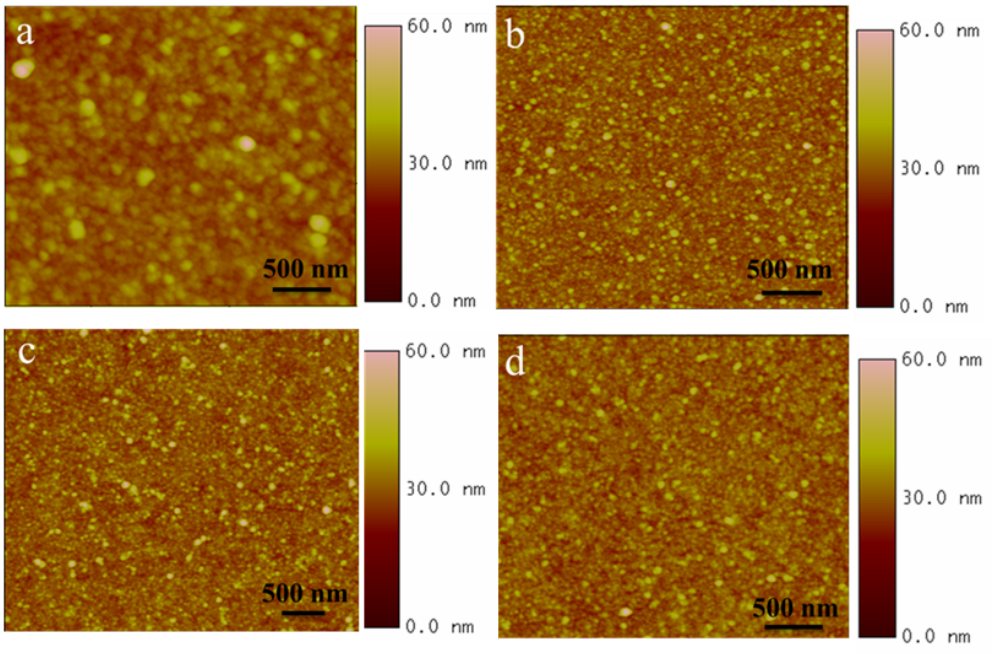

Fig. S11. AFM images of four composite films $[PEI/PW/Ruphen/PSS]_3/PEI/PW/Ruphen$ on quartz substrates: (a) PW_{12}; (b) P_2W_{18}; (c) P_5W_{30} and (d) P_8W_{48} in scanning range of 5 micrometer.

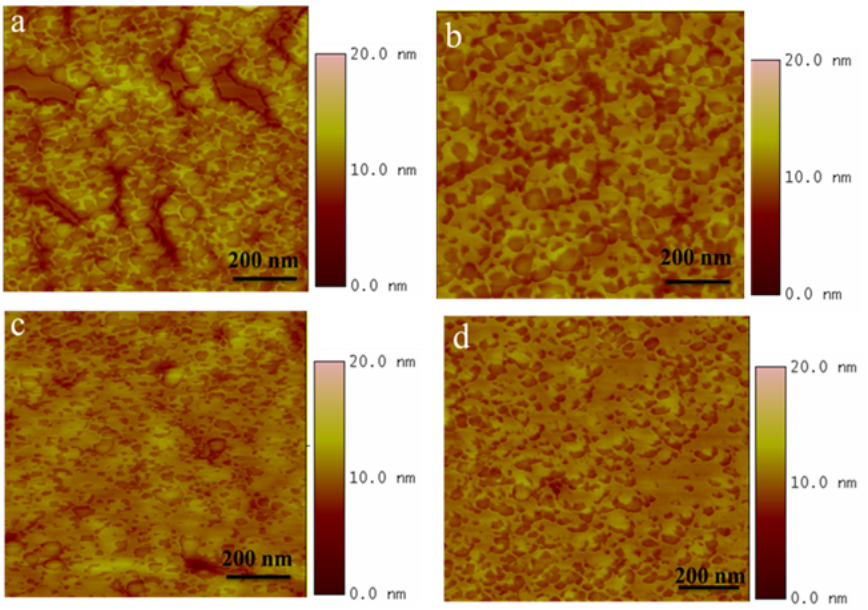

Fig. S12. AFM images of four composite films $[PEI/PW]_1$ on quartz substrates: (a) PW_{12}; (b) P_2W_{18}; (c) P_5W_{30} and (d) P_8W_{48} in scanning range of 1 micrometer.

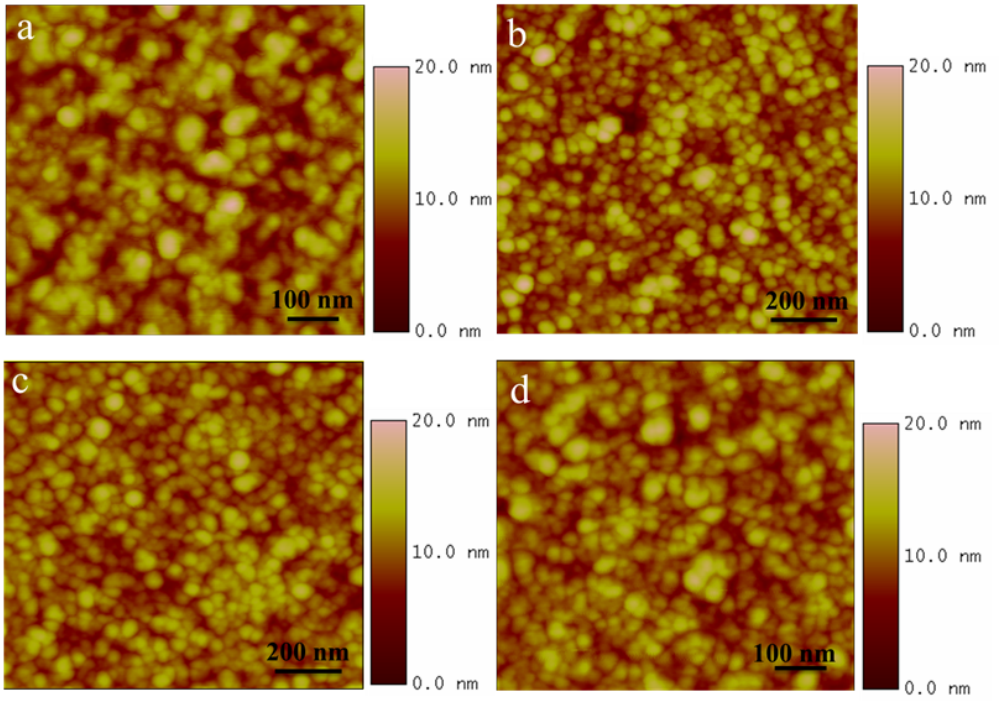

Fig. S13. AFM images of four composite films [PEI/PW/Ru(phen)/PSS]$_3$/PEI/PW on quartz substrates: (a) PW_{12}; (b) P_2W_{18}; (c) P_5W_{30} and (d) P_8W_{48} in scanning range of 1 micrometer..

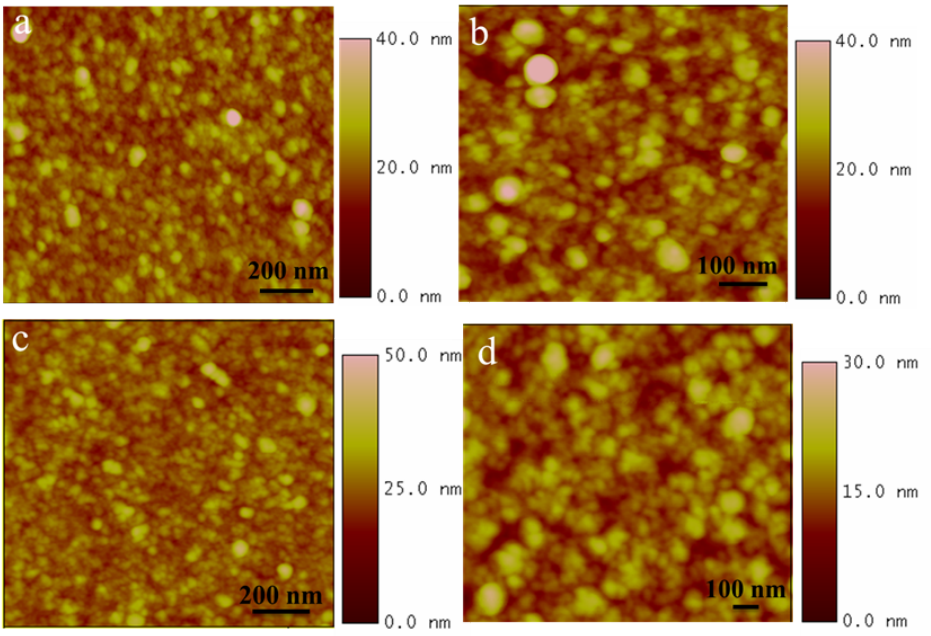

Fig. S14. AFM images of four composite films [PEI/PW/Ruphen/PSS]$_3$/PEI/PW/Ruphen on quartz substrates: (a) PW_{12}; (b) P_2W_{18}; (c) P_5W_{30} and (d) P_8W_{48} in scanning range of 1 micrometer..

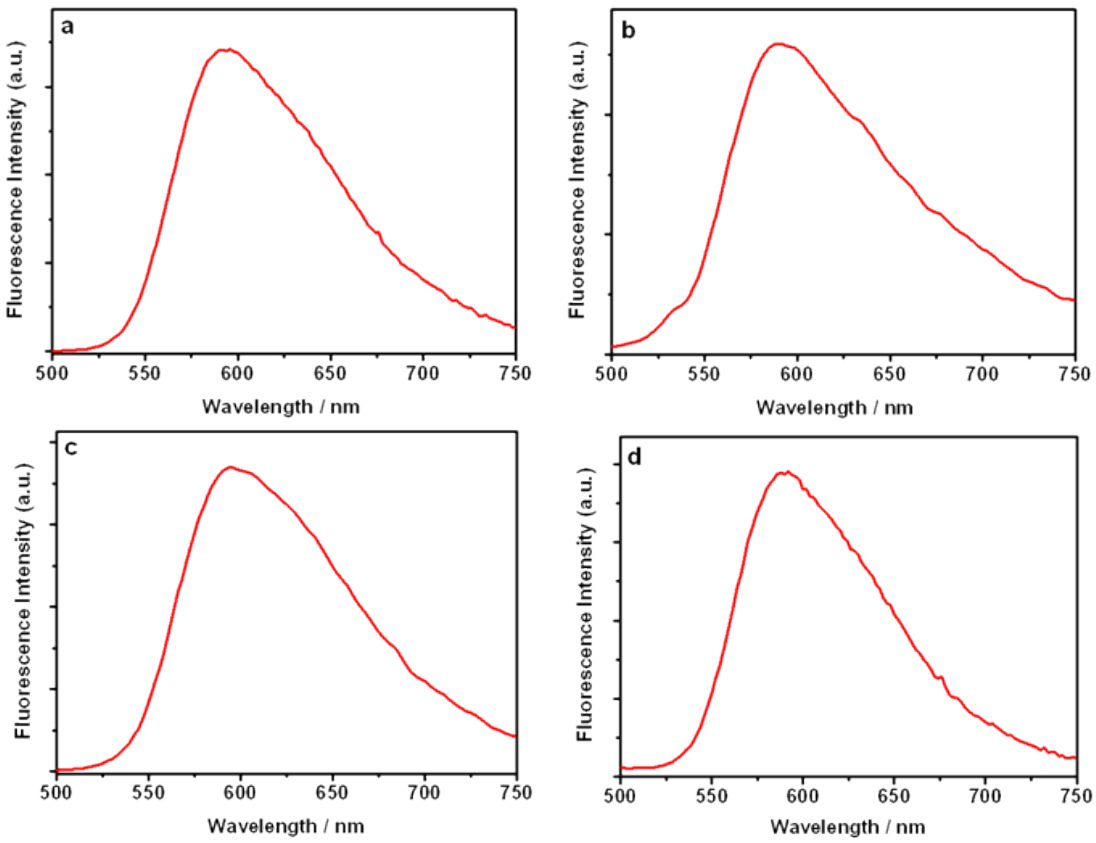

Fig. S15. Fluorescence spectra (λ_{ex} = 450 nm) of four composite films $(PEI/PW/Ruphen/PSS)_{15}$ on ITO in 0.5 M Na_2SO_4/H_2SO_4 (pH 2.5): (a) PW_{12}; (b) P_2W_{18}; (c) P_5W_{30}; (d) P_8W_{48}.

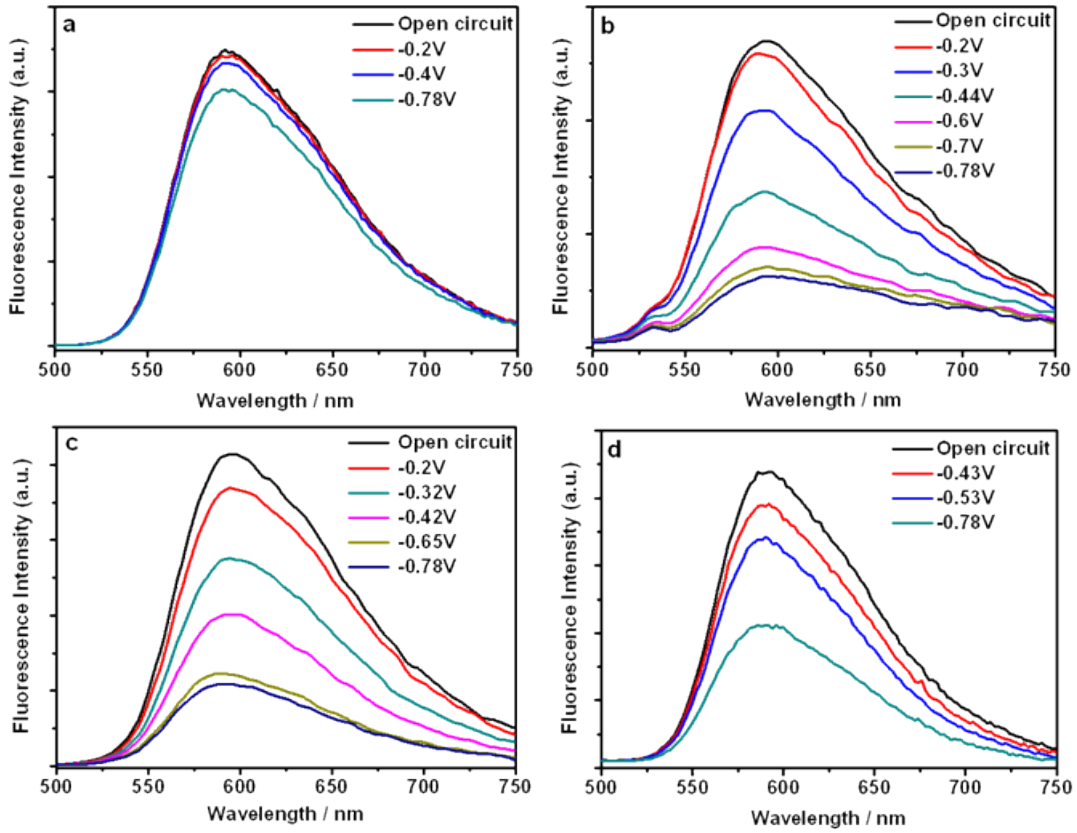

Fig. S16. Luminescence spectra of four composite films $(PEI/PW/Ruphen/PSS)_{15}$ on ITO in 0.5 M Na_2SO_4/H_2SO_4 (pH 2.5) at different applied reduced potentials: (a) PW_{12}; (b) P_2W_{18}; (c) P_5W_{30}; (d) P_8W_{48}.

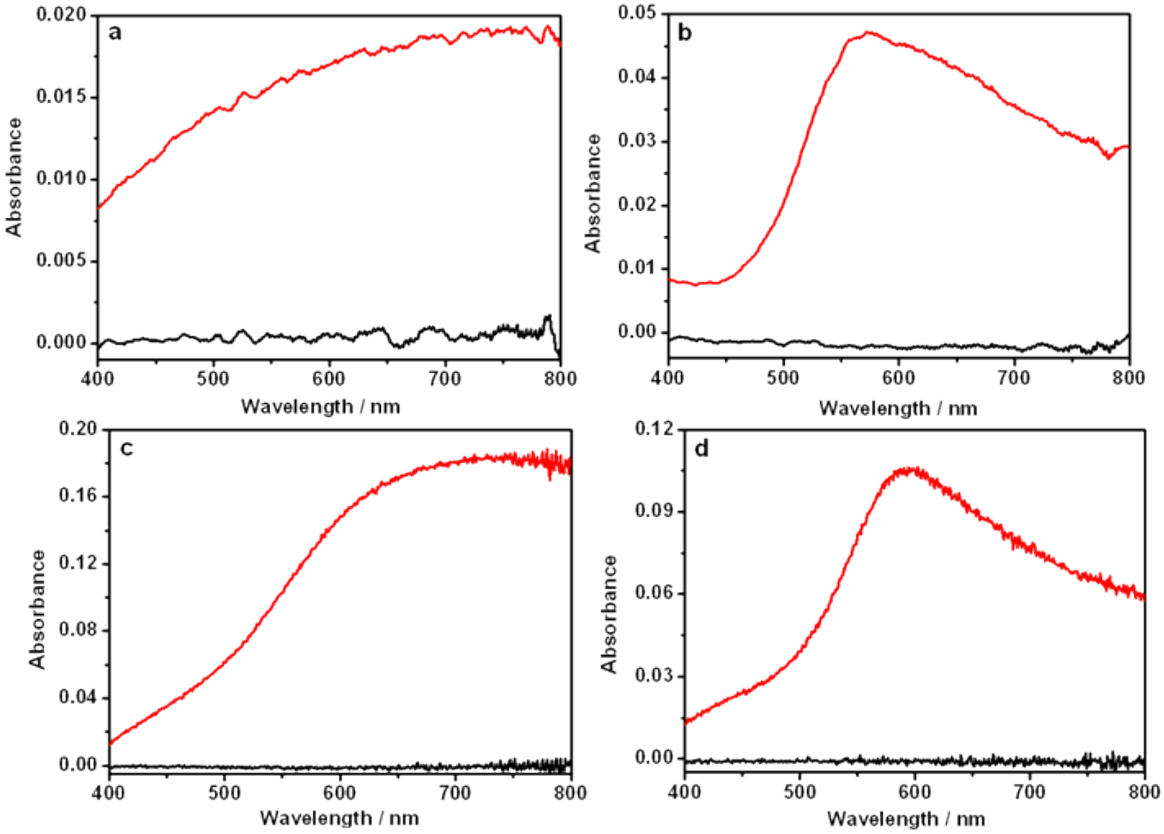

Fig. S17. Absorption spectra of four composite films $(PEI/PW/Ruphen/PSS)_{15}$ on ITO in 0.5 M Na_2SO_4/H_2SO_4 (pH 2.5) under open circuit (black curves) and at applied potential of -0.78 V (red curves). (a) PW_{12}; (b) P_2W_{18}; (c) P_5W_{30}; (d) P_8W_{48}.

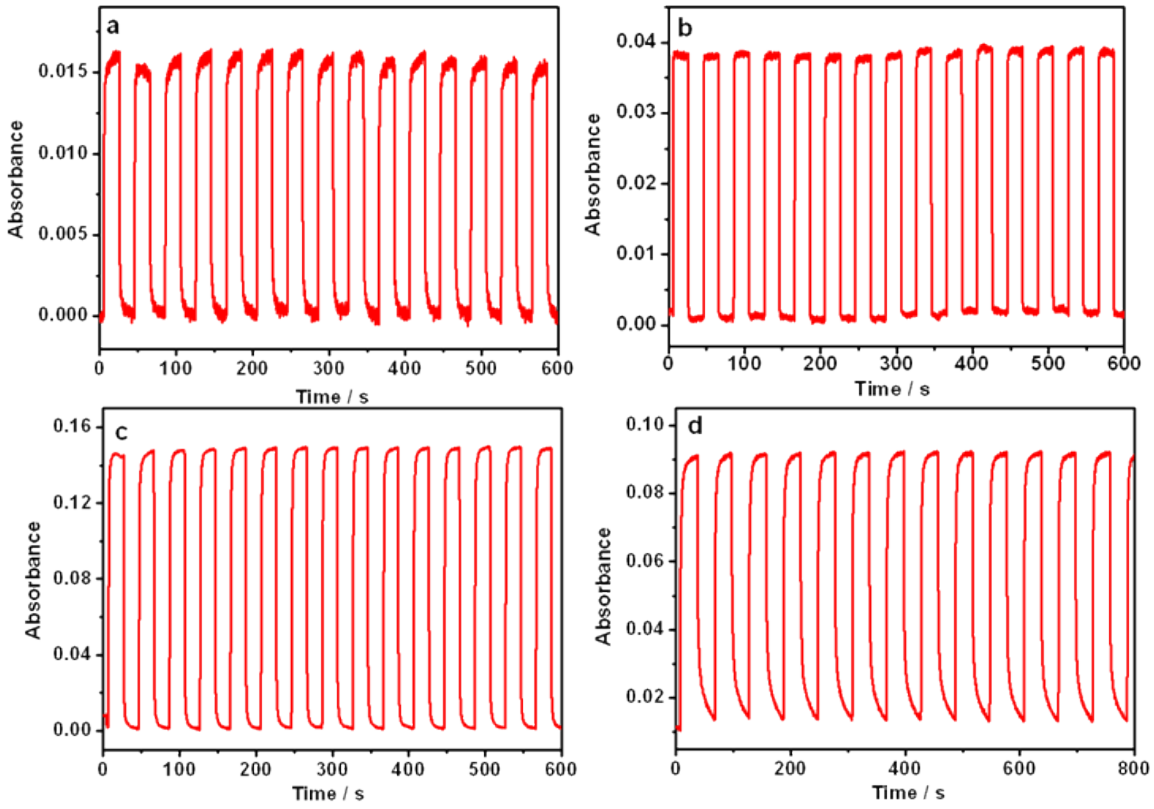

Fig. S18. Absorbance at 650 nm of four composite films (a) $(PEI/PW_{12}/Ruphen/PSS)_8$; (b) $(PEI/P_2W_{18}/Ruphen/PSS)_8$; (c) $(PEI/P_5W_{30}/Ruphen/PSS)_8$ and (d) $(PEI/P_8W_{48}/Ruphen/PSS)_8$ on ITO during subsequent double-potential steps from -0.7 to 0.7 V in 0.5 M Na_2SO_4/H_2SO_4 (pH 2.5) solutions.

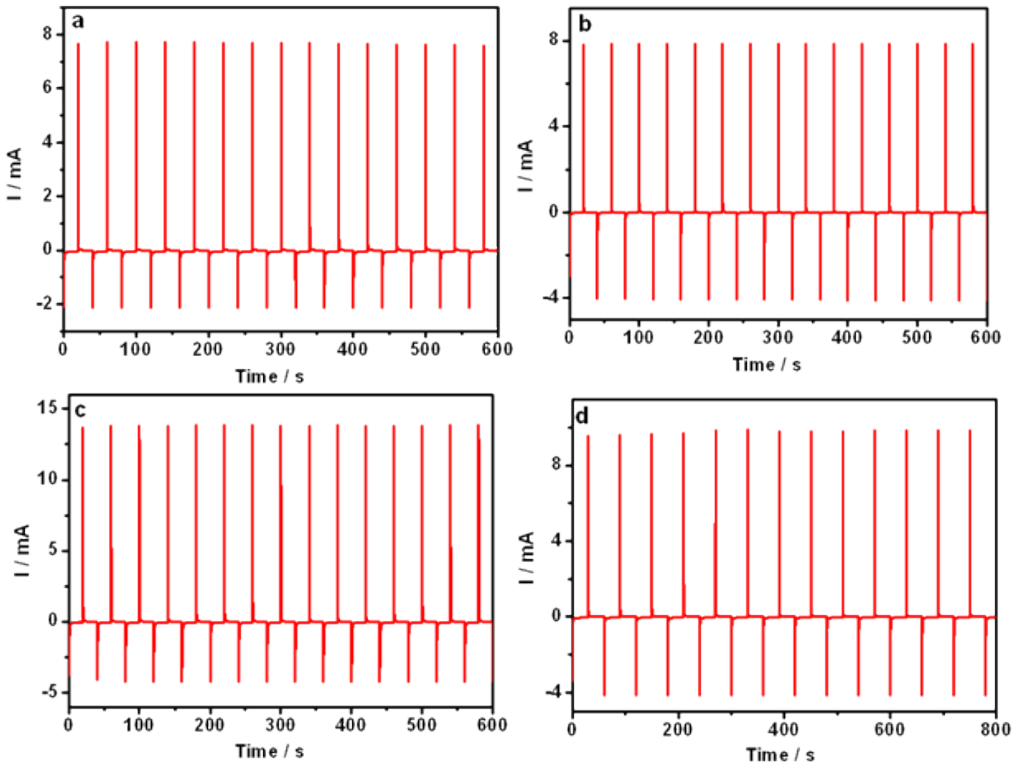

Fig. S19. Currents of four composite films (a) $(PEI/PW_{12}/Ruphen/PSS)_8$; (b) $(PEI/P_2W_{18}/Ruphen/PSS)_8$; (c) $(PEI/P_5W_{30}/Ruphen/PSS)_8$ and (d) $(PEI/P_8W_{48}/Ruphen/PSS)_8$ on ITO during subsequent double-potential steps from -0.7 to 0.7 V in 0.5 M Na_2SO_4/H_2SO_4 (pH 2.5) solutions.

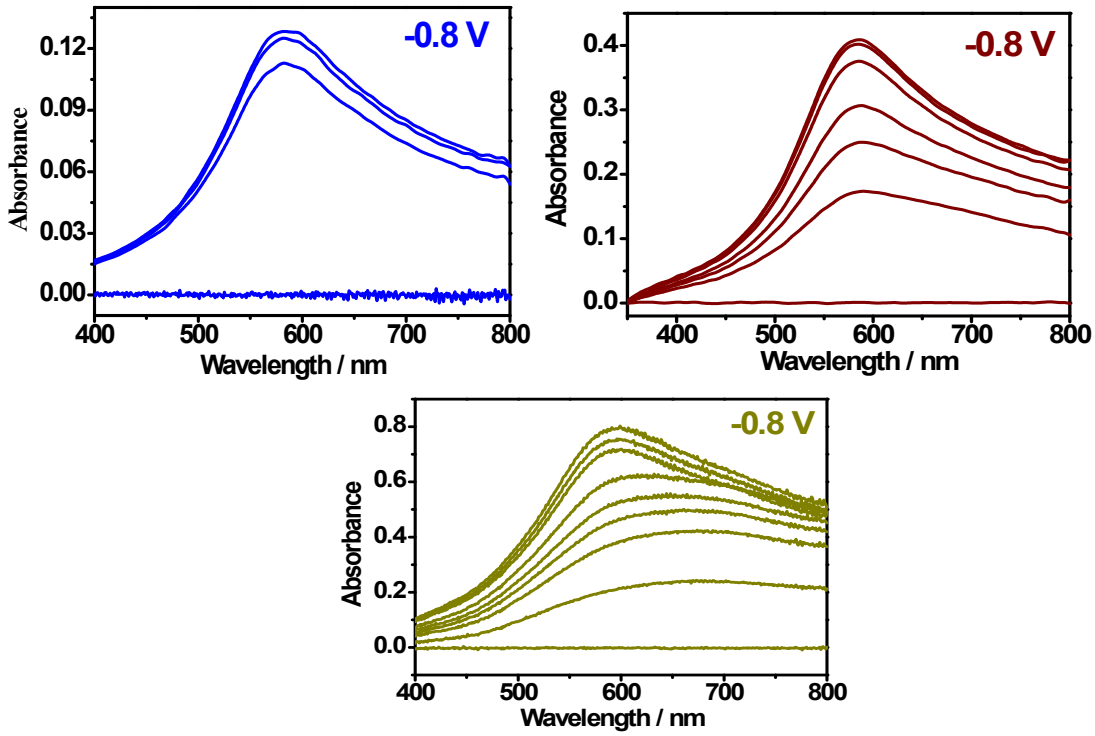

Fig. S20. UV-visible absorption spectra of three composite films $[PEI/P_8W_{48}/Ruphen/PSS]_{23}$ (upper left), $[(PEI/P_8W_{48})_4/Ruphen/PSS]_{12}$ (upper right) and $[(PEI/P_8W_{48})_7/Ruphen/PSS]_{10}(PEI/P_8W_{48})_7$ (bottom) on ITO in 0.5 M H_2SO_4/Li_2SO_4 (pH = 3) vs. the electrochemical reduction time when applied a reduction potential of −0.8 V.